The Plant Cell, Vol. 6, 1713–1729, December 1994 © 1994 American Society of Plant Physiologists

Cell Differentiation and Morphogenesis Are Uncoupled in Arabidopsis *raspberry* Embryos

Ramin Yadegari,[a] Genaro R. de Paiva,[a,1] Thomas Laux,[a,2] Anna M. Koltunow,[a,3] Nestor Apuya,[b,4] J. Lynn Zimmerman,[b] Robert L. Fischer,[c] John J. Harada,[d] and Robert B. Goldberg [a,5]

[a] Department of Biology, University of California, Los Angeles, California 90024-1606
[b] Department of Biology, University of Maryland Baltimore County, Baltimore, Maryland 21228
[c] Department of Plant Biology, University of California, Berkeley, California 94720
[d] Section of Plant Biology, Division of Biological Sciences, University of California, Davis, California 95616

We identified two Arabidopsis embryo mutants, designated as *raspberry1* and *raspberry2*, by screening T-DNA–mutagenized Arabidopsis lines. Embryogenesis in these mutants is indistinguishable from that of wild-type plants until the late-globular stage, after which *raspberry1* and *raspberry2* embryos fail to undergo the transition to heart stage, remain globular shaped, and proliferate an enlarged suspensor region. *raspberry1* and *raspberry2* embryo-proper regions enlarge during embryogenesis, become highly vacuolate, and display prominent convex, or "raspberry-like," protuberances on their outer cell layers. In situ hybridization studies with several embryo cell–specific mRNA probes indicated that the *raspberry1* and *raspberry2* embryo-proper regions differentiate tissue layers in their correct spatial contexts and that the regulation of cell-specific genes within these layers is normal. Surprisingly, a similar spatial and temporal pattern of mRNA accumulation occurs within the enlarged suspensor region of *raspberry1* and *raspberry2* embryos, suggesting that a defect in embryo-proper morphogenesis can cause the suspensor to take on an embryo-proper–like state and differentiate a radial tissue–type axis. We conclude that cell differentiation can occur in the absence of both organ formation and morphogenesis during plant embryogenesis and that interactions occur between the embryo-proper and suspensor regions.

INTRODUCTION

A mature plant embryo contains two specialized organ systems—the axis and cotyledon (Raven et al., 1992). The axis consists of the hypocotyl and radicle regions and contains the shoot and root meristems that are responsible for differentiating organ systems of the postembryonic plant. The cotyledon, on the other hand, is a terminally differentiated structure that functions in the accumulation of storage reserves that are consumed by the germinating seedling after seed dormancy ends. Each embryonic organ system has three specialized tissue layers—epidermis, storage parenchyma, and vascular—which are organized spatially along a radial axis and express distinct gene sets (Goldberg et al., 1989, 1994). For example, storage protein genes are transcriptionally activated within the parenchyma cells, while lipid transfer protein genes are expressed in the epidermal cell layer (Goldberg et al., 1989; Perez-Grau and Goldberg, 1989; Guerche et al., 1990; Sterk et al., 1991). The precise mechanisms responsible for the differentiation of embryonic cell layers and the selective transcription of gene sets within these layers are not known.

A major question is whether the cell types present in a mature embryo can form in the absence of morphogenetic events that give rise to the embryonic organ systems. That is, can the primary embryonic cell layers that are specified in the globular embryo differentiate into the specialized tissues of the mature embryo in the absence of cotyledon and axis formation? The identification of Arabidopsis embryo mutants that lack either cotyledon or axis regions suggests that this is the case (Mayer et al., 1991). For example, *monopteros* lacks a normal axis region but forms cotyledons that have epidermal, ground meristem, and vascular cell layers (Mayer et al., 1991; Berleth and Jürgens, 1993). Similarly, *gurke* lacks cotyledons but has a normal radial tissue–type axis in its hypocotyl region (Mayer et al., 1991). By contrast, mutant embryos such as *knolle*, which fail to specify a normal epidermal layer, have major morphological defects (Mayer et al., 1991). Thus, histodifferentiation occurs independently within each embryonic region and can take place in embryos with defects in

[1] Current address: Centro Nacional de Recursos e Biotecnologia, C.P. 102372, Brasilia, DF, 70770, Brazil.
[2] Current address: Lehrstuhl für Genetik, Universität München, D-8000 München 19, Germany.
[3] Current address: CSIRO Division of Horticulture, GPO Box 350, Adelaide, South Australia 5001, Australia.
[4] Current address: Department of Biology, University of California, Los Angeles, CA 90024-1606.
[5] To whom correspondence should be addressed.

morphogenesis. Morphological development, however, is severely affected in embryos that have defects in tissue differentiation.

We screened T-DNA–mutagenized Arabidopsis lines (Feldmann, 1991; Forsthoefel et al., 1992) for mutations that affect embryo development. We uncovered two mutants, designated as *raspberry1* and *raspberry2*, that remain globular shaped, fail to form axis and cotyledon organ systems, and have an enlarged, multi-tiered suspensor region that persists throughout embryogenesis. In situ hybridization experiments with several cell-specific mRNAs indicated that *raspberry1* and *raspberry2* embryo-proper regions differentiate cell layers in their correct spatial contexts and that gene regulation in these cell layers is normal. Surprisingly, the enlarged *raspberry1* and *raspberry2* suspensor regions have cell type–specific mRNA localization patterns similar to those observed in the embryo proper. Our results indicate that (1) the primary embryonic cell layers can become specialized in the absence of organ formation, (2) the suspensor has the potential to differentiate an embryo-proper–like radial tissue axis, and (3) interactions occur between the embryo-proper and suspensor regions. We conclude that cells formed during early embryogenesis are programmed to follow a specific differentiation pathway and can regulate gene sets in their proper temporal and spatial contexts independently of the morphogenetic events that give rise to an embryo with a normal body pattern.

RESULTS

raspberry Mutants Are Identified in T-DNA–Mutagenized Arabidopsis Lines

We screened 5822 T-DNA–mutagenized Arabidopsis lines for mutations that affect embryo development (see Methods). Table 1 shows that 66 lines produced seeds that contained mutant embryos with a range of phenotypic abnormalities. Wild-type and mutant embryos segregated with a 3:1 ratio in the siliques of each line, indicating that the defects in embryogenesis were caused by recessive mutations in zygotically acting genes (data not shown). DNA gel blot analysis and kanamycin resistance tests on wild-type and heterozygous plants that segregated within each mutant family indicated that approximately one-third of the embryo mutations were linked closely with T-DNA insertions (data not shown). As summarized in Table 1, the largest class of mutations caused the embryos to remain globular shaped and failed to differentiate cotyledon and axis organ systems. We chose two mutants in this class, *raspberry1* and *raspberry2*, for further study.

Reciprocal crosses between *raspberry1* and *raspberry2* heterozygous plants indicated that the two mutations belong to separate complementation groups (data not shown). *raspberry2* was not tagged with T-DNA, as indicated by DNA gel blot analyses of eight wild-type and heterozygous segregants with a T-DNA right-border probe (data not shown). By contrast, DNA gel blot analysis of 32 segregants suggested that *raspberry1* was tightly linked to the T-DNA. To show more precisely linkage of the *raspberry1* mutation to the T-DNA, 170 heterozygous T_4 plants with 25% defective T_5 seeds were shown to be kanamycin resistant (data not shown). Genetic mapping studies indicated that the *raspberry1* gene is located at position 22 on chromosome 3 (D.W. Meinke, personal communication).

Table 1. Embryo Mutants Obtained from T-DNA–Mutagenized Arabidopsis Lines

Class	Number of Mutants
Preglobular	14
Globular[a]	29
Transition/heart	7
Cotyledon[b]	6
Pattern[c]	6
Fusca[d]	2
Other[e]	2

[a] Only one mutant (*stout*) in this class did not exhibit the "raspberry" phenotype and had a phenotype similar to a wild-type globular embryo (Figure 7).
[b] This class includes a group of mutants that arrest beyond the heart stage but that exhibit a variety of morphological abnormalities.
[c] This class either lacks or has defective cotyledon or axis organ systems (Mayer et al., 1991).
[d] *fusca* embryos are not defective morphologically; however, they accumulate anthocyanins in their cotyledons at the maturation stage of embryo development (Castle et al., 1993).
[e] Unresolved phenotypes.

raspberry Embryos Fail to Form Organs and Proliferate an Enlarged Suspensor

We compared the phenotypes of *raspberry* and wild-type embryos using light microscopy. As shown in Figures 1A and 1B, a wild-type, globular-stage embryo contained a spherical embryo proper attached to a suspensor with seven to nine cells arranged in a linear file (Mansfield and Briarty, 1991). At this stage of development (mid- to late-globular stage), the embryo proper contained three primary tissue layers—protoderm, ground meristem, and procambium (Figure 1B). Suspensor cells were not distinct from each other histologically, except for those in the hypophysis region contiguous with the embryo proper (Figures 1A and 1B). The wild-type, late-maturation stage embryo shown in Figure 1C had differentiated axis and cotyledon organ systems that contained specialized epidermal, vascular, and storage parenchymal tissue layers (Mansfield and Briarty, 1992). The suspensor, which senesces after the heart stage (Mansfield and Briarty, 1991, 1992), was absent.

We characterized *raspberry* embryo phenotypes at a developmental period when wild-type embryos within the same silique were in late maturation (Figure 1C). Figures 1D to 1I show that *raspberry1* and *raspberry2* embryos had similar

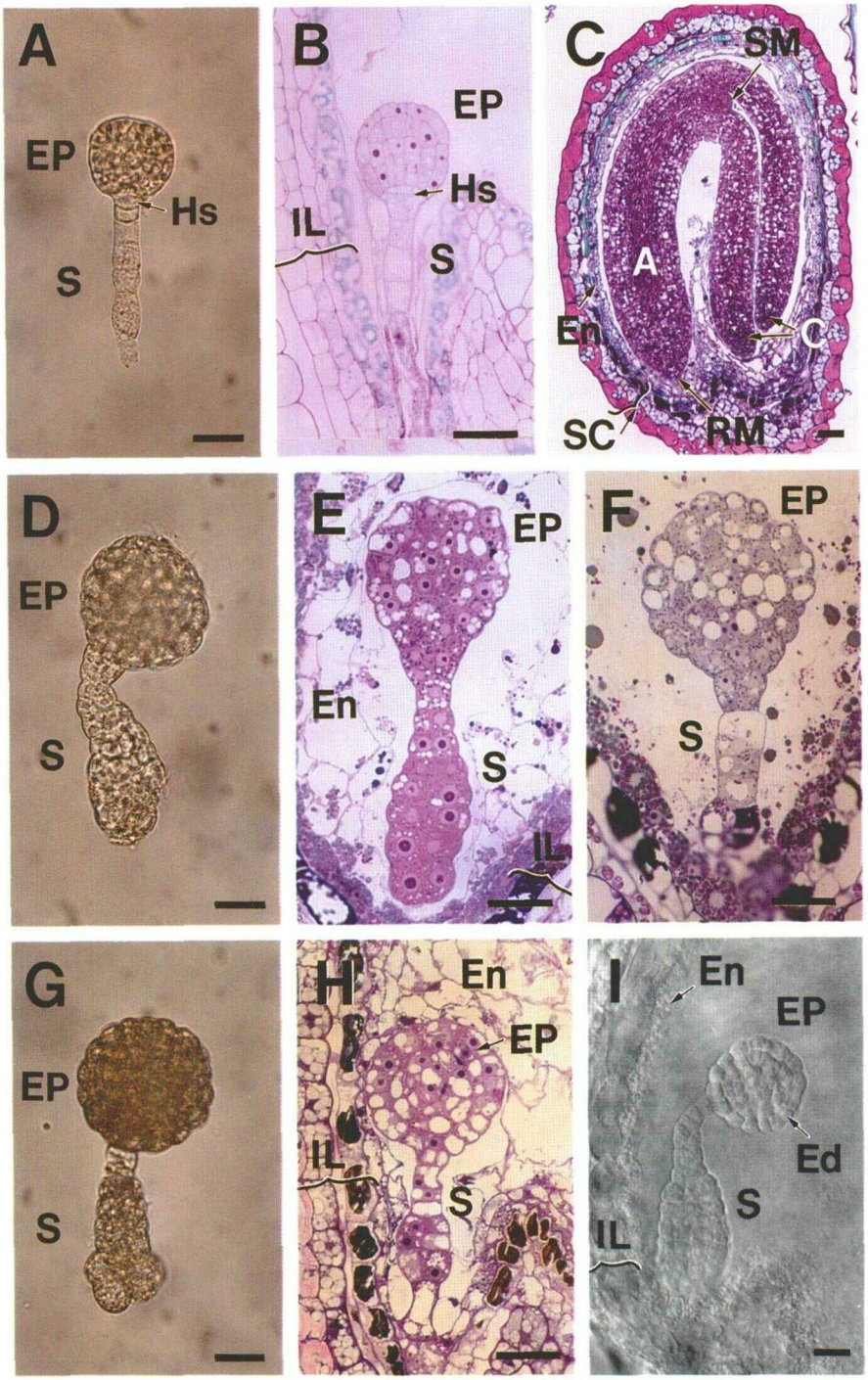

Figure 1. Phenotypes of *raspberry* Embryos.

(A) to **(C)** Wild-type embryos at the globular stage are shown in **(A)** and **(B)** and at a late-maturation stage in **(C)**. Whole-mount embryo **(A)** and longitudinal embryo sections (**[B]** and **[C]**) were photographed by bright-field microscopy.

(D) to **(F)** *raspberry2* embryos taken from seeds at a developmental stage equivalent to that shown in **(C)** for wild-type embryos. Whole-mount embryo **(D)** and longitudinal embryo sections (**[E]** and **[F]**) were photographed by bright-field microscopy.

(G) to **(I)** *raspberry1* embryos taken from seeds at a developmental stage equivalent to that of the wild-type embryo shown in **(C)**. Whole-mount embryo **(G)** and longitudinal embryo sections **(H)** were photographed by bright-field microscopy. The whole-mount embryo **(I)** was photographed by Nomarski optics.

A, axis; C, cotyledon; Ed, epidermis; En, endosperm; EP, embryo proper; Hs, hypophysis; IL, integument layers; RM, root meristem; S, suspensor, SC, seed coat; SM, shoot meristem. Bars = 25 μm.

morphological characteristics. These mutants remained globular shaped, proliferated an enlarged suspensor with several cell layers, and were embedded in a cellularized endosperm that was similar to that found in wild-type seeds (Figures 1C, 1E, 1H, and 1I). In contrast to wild-type embryos at the globular stage (Figures 1A and 1B), *raspberry* embryos contained highly vacuolated, irregularly shaped cells and had convex, "raspberry-like" protuberances on their outer cell layers (Figures 1D to 1I). *raspberry* embryos had ~250 cells (embryo-proper region) and were approximately twofold larger than wild-type embryos at the late-globular stage as a consequence of both cell proliferation and expansion events (compare Figures 1A and 1D; data not shown). Distinct ground meristem and procambium cell layers could not be identified within the interior cell mass by histological inspection (Figures 1E, 1F, 1H, and 1I); nor were there apparent root or shoot meristematic tissues (Figure 1I). Only an outer ring of epidermal-like cells was apparent within the *raspberry1* and *raspberry2* embryo-proper regions (Figure 1I). Figures 1D to 1I show that *raspberry* suspensor regions did not have a stereotyped morphology and varied in both size and shape between individual embryos (e.g., compare Figures 1E and 1F). The proliferation of *raspberry* suspensor cells was greatest at the micropylar end, where attachment occurred to the embryo sac (Figures 1D to 1I). Together, these data show that *raspberry1* and *raspberry2* embryos fail to undergo organ formation, remain globular shaped, and have suspensors that undergo extensive cell divisions in abnormal planes.

Raspberry-like Protuberances Are Late-Embryogenesis Markers

We characterized *raspberry* embryos in greater detail by using scanning and transmission electron microscopy. Figures 2A and 2B show that *raspberry1* (Figure 2B) and *raspberry2* (Figure 2A) embryo-proper regions contained a mosaic of irregularly sized protuberances projecting outward from the embryo surfaces. These convex protuberances were also present on the outer surfaces of mutant suspensor regions (Figures 2A and 2B). Figure 2C shows that the surface of a wild-type embryo at the late-globular stage was relatively smooth. By contrast, Figures 2D and 2E show that a wild-type, late-maturation stage embryo had convex protuberances analogous to those observed for *raspberry* embryos (Figures 1A and 1B) on the outer surfaces of both the axis and cotyledon regions (Figure 2D).

The transmission electron micrographs shown in Figures 2F and 2G indicate that the convex protuberances on both *raspberry* embryos (Figure 2F) and late-maturation stage, wild-type embryos (Figure 2G) were due to outward projections along the entire exterior cell wall surface and that these projections varied in size and shape from cell to cell. Cells around the entire perimeter of *raspberry* embryo-proper regions contained convex projections; that is, protuberances were present on cells in both the micropylar and chalazal regions (data not shown).

The cells of *raspberry* embryos contained large vacuoles that varied in size, had small amounts of electron-dense material within them, and resembled vacuoles present in wild-type embryos just prior to storage protein deposition (Figure 2F; Mansfield and Briarty, 1992). Similar types of vacuoles were observed in both embryo-proper and suspensor cells (Figure 2F; and data not shown). Numerous electron-dense bodies analogous to those observed in wild-type embryos at the torpedo stage were also present in *raspberry* cells (Figure 2F; Mansfield and Briarty, 1991). The function of these bodies is not known (Mansfield and Briarty, 1992). Mature chloroplasts were not present within *raspberry* cells, which was consistent with the white color of *raspberry1* and *raspberry2* embryos (Figures 1D and 1G); nor were there detectable lipid bodies or mature protein bodies (Figure 2F). By contrast, the cells of wild-type, late-maturation stage embryos contained numerous lipid bodies, chloroplasts, and protein bodies with large amounts of storage proteins within them (Figure 2G; Mansfield and Briarty, 1992). As shown in Figure 2H, wild-type embryos at the early-heart stage did not contain prominent vacuoles, lipid bodies, protein bodies, or chloroplasts. Together, these data indicate that the cellular features of *raspberry* embryos more closely resemble those of wild-type embryos at the maturation stage than those of globular- or heart-stage embryos and that the presence of vacuoles and "raspberry-like" protuberances are late-embryogenesis markers.

raspberry Embryos Develop Normally until the Transition Stage

We determined the earliest stage at which *raspberry1* embryos showed morphological defects by examining longitudinal sections of heterozygous siliques at different developmental periods for abnormal embryos that represented 25% of the embryo population. We examined older siliques containing well-developed *raspberry1* and maturation-stage embryos first (Figures 1C and 1H) and then worked backward developmentally to identify a silique stage that did not contain 25% abnormal-looking embryos. Figures 3A to 3D show bright-field photographs of representative embryos from young heterozygous siliques. Approximately 20 individual embryos were examined within each silique, and no morphological or histological differences were observed among populations of early-globular stage embryos (Figures 3A and 3C) and late-globular stage embryos (Figures 3B and 3D) at this level of resolution. Nor were there observable differences in endosperm development between individual seeds within these siliques—a free nuclear endosperm formed early in seed development (Figures 3A and 3C), and this endosperm became cellularized at the late-globular stage (Figures 3B and 3D). By contrast, Figures 3E and 3F show that mutant embryos (Figure 3F) were observed in siliques that contained wild-type embryos at the transition stage (Figure 3E). Mutant embryos were identified because they retained a globular-shaped, embryo-proper region, had "raspberry-like" protuberances, and

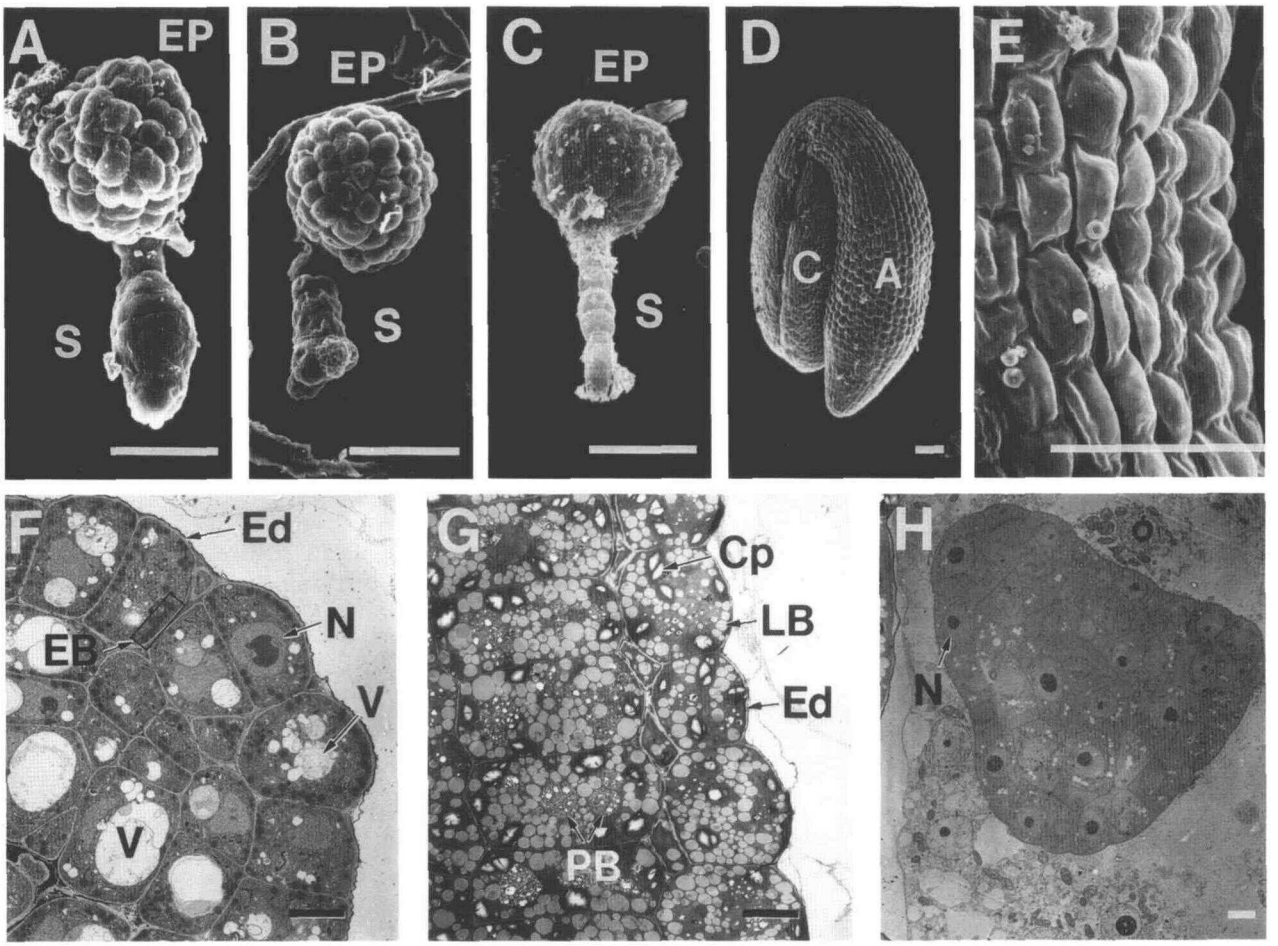

Figure 2. Electron Microscopy of *raspberry* Embryos.

(A) to **(E)** Scanning electron micrographs of a *raspberry2* embryo **(A)**, a *raspberry1* embryo **(B)**, and wild-type embryos at the late-globular stage **(C)** and late-maturation stage (**[D]** and **[E]**). The micrograph shown in **(E)** represents a higher magnification of axis cells from the late-maturation stage embryo shown in **(D)**. *raspberry* embryos were harvested from seeds at a stage when wild-type embryos within the same silique were at the late-maturation stage **(D)**.

(F) to **(H)** Transmission electron micrographs of a *raspberry1* embryo **(F)** and wild-type embryos at the late-maturation stage **(G)**, and the early-heart stage **(H)**. The *raspberry1* embryo shown in **(F)** was harvested from a mutant seed at a stage when wild-type seeds within the same silique contained late-maturation stage embryos **(D)**.

A, axis; C, cotyledon; Cp, chloroplast; EB, electron-dense body; Ed, epidermis; EP, embryo proper; LB, lipid body; N, nucleus; PB, protein body; S, suspensor; V, vacuole. Bars = 33 μm in **(A)** to **(E)**, 5 μm in **(F)** to **(H)**.

represented 25% of the embryos in these siliques (Figure 3F). Figures 3F to 3J show that mutant embryos (Figures 3I and 3J) were present within developmentally advanced siliques containing either heart-stage embryos (Figure 3G) or maturation-stage embryos (Figure 3H). *raspberry1* embryo-proper regions increased in size during this period due to both cell division and enlargement events (Figures 3I and 3J), and suspensor cell proliferation was most pronounced during the terminal stages of embryo development (data not shown). In contrast to the peripheral endosperm that lined the interior of seeds containing maturation-stage embryos (Figure 3H), endosperm cells in seeds containing *raspberry1* embryos were concentrated primarily around the suspensor (Figure 3J).

We investigated *raspberry1* embryo development at stages immediately after fertilization to determine whether subtle changes occurred in cell division and/or differentiation patterns. A total of 17 heterozygous siliques containing embryos from the zygote stage to the mid-heart stage were examined using Nomarski interference optics (see Methods). No differences were observed among either the zygote or the two-cell embryo populations of very young siliques, indicating that the first zygotic division was unaffected by the *raspberry1* mutation

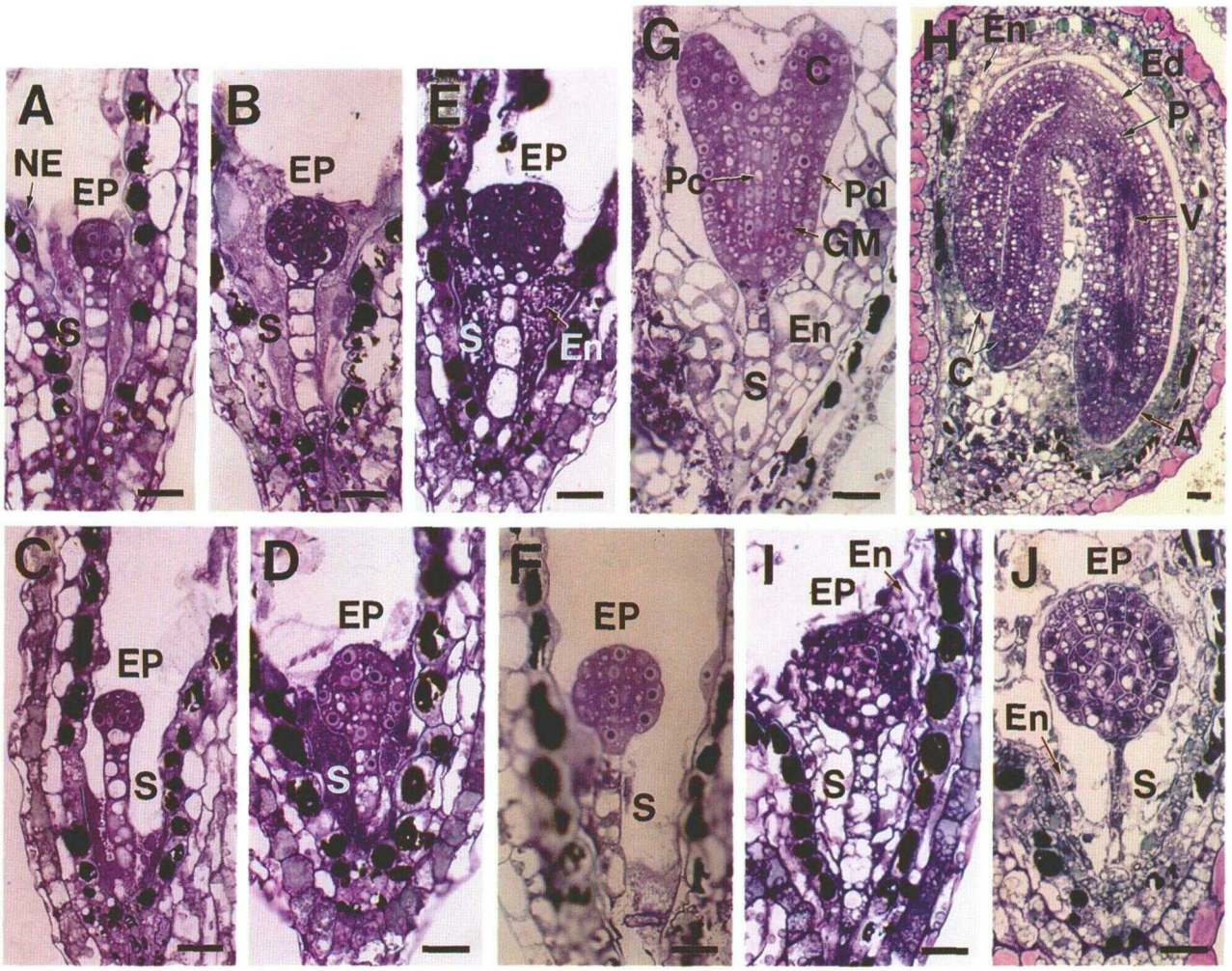

Figure 3. Development of *raspberry1* Embryos.

Siliques from a heterozygous plant were staged, fixed, embedded in plastic, and sliced into sections (1 to 2 μm; see Methods).
(A) to **(D)** Bright-field photographs of globular embryos from heterozygous +/*raspberry1* siliques. Embryos at the early-globular stage (**[A]** and **[C]**) and the late-globular stage (**[B]** and **[D]**) are shown.
(E) and **(F)** Bright-field photographs of a transition-stage, wild-type embryo **(E)** and a *raspberry1* embryo **(F)** within heterozygous +/*raspberry1* siliques.
(G) and **(H)** Bright-field photographs of developing wild-type embryos from heterozygous +/*raspberry1* siliques. A late-heart stage embryo is shown in **(G)**, and a late-maturation stage embryo is shown in **(H)**.
(I) and **(J)** Bright-field photographs of developing *raspberry1* embryos. Embryos contained within the same siliques as wild-type embryos are shown in **(G)** and **(H)**.
A, axis; C, cotyledon; Ed, epidermis; En, endosperm; EP, embryo proper; GM, ground meristem; NE, nuclear endosperm; P, storage parenchyma; Pc, procambium; Pd, protoderm; S, suspensor; V, vascular tissue. Bars = 19 μm.

(data not shown). Figure 4 shows that we could not distinguish between mutant and wild-type embryos prior to the transition stage of development (Figures 4A to 4E). Stereotyped cell division patterns were observed within both the embryo-proper and suspensor regions, a protoderm was visible at the 16-cell stage, and a normal-looking hypophysis formed (Figures 4A to 4E). By contrast, *raspberry1* embryos were readily visible within siliques that contained either transition- or heart-stage embryos (Figures 4F to 4K). Enlargement of *raspberry1* embryos occurred but was not accompanied by cotyledon or axis differentiation. Cell divisions did take place within the hypophysis; however, these divisions caused this region to become indistinguishable from the ring of epidermal-like cells surrounding the embryo proper (Figure 1I and Figures 2I to 2K). Taken together, these data indicate that the early stages of *raspberry1* embryo development appear normal but that *raspberry1*

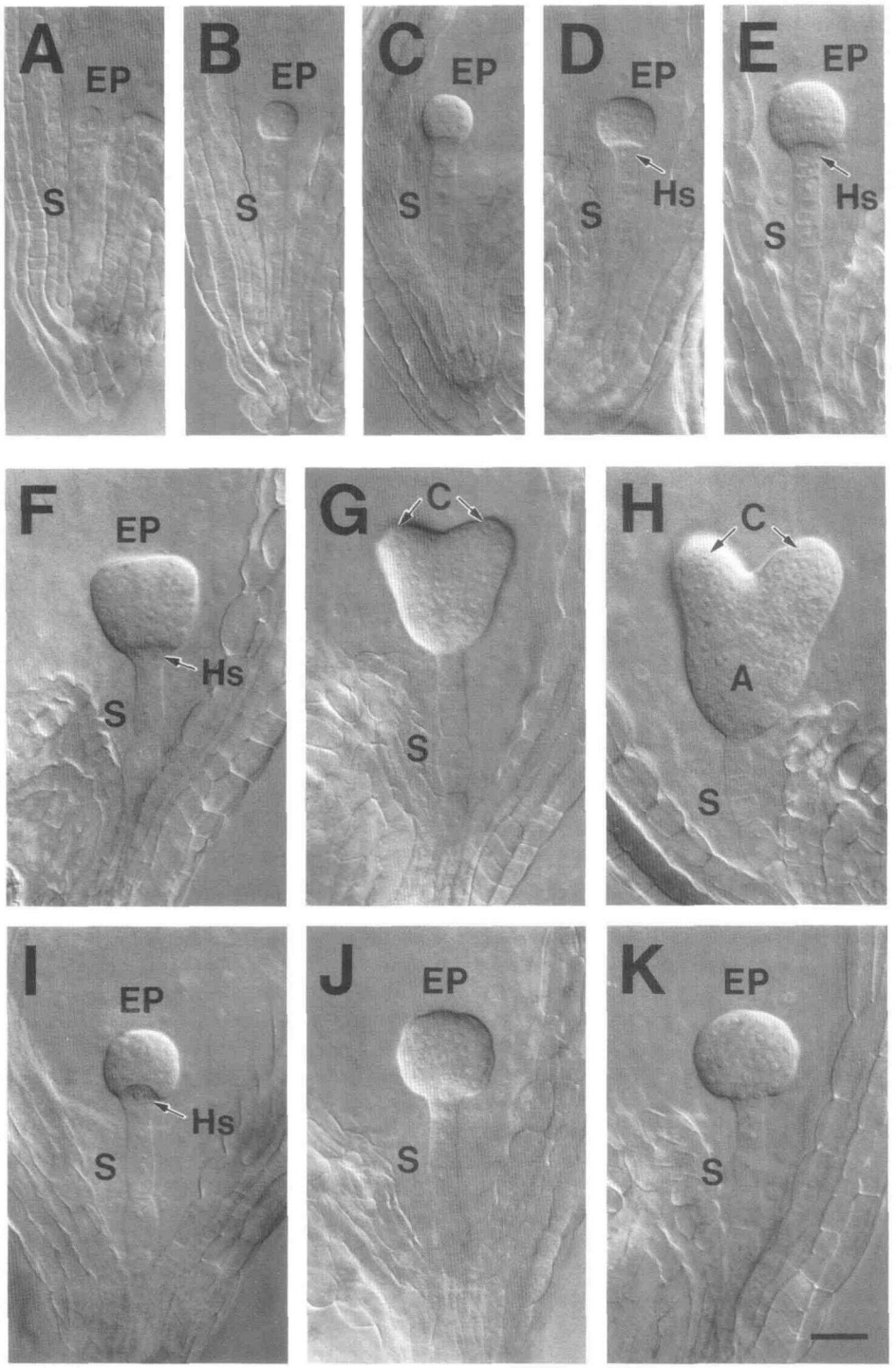

Figure 4. Early Development of *raspberry1* Embryos.

Siliques from heterozygous plants were staged, fixed, and cleared. Bright-field photographs of embryos were taken using Nomarski optics (see Methods).
(A) to **(E)** Photographs of preglobular and globular embryos from heterozygous +/*raspberry1* siliques. Embryos at the two/four-cell stage **(A)**, eight-cell stage **(B)**, 16-cell stage **(C)**, early-globular stage **(D)**, and mid-globular stage **(E)** are shown.
(F) to **(H)** Photographs of developing wild-type embryos from heterozygous +/*raspberry1* siliques. Embryos at the transition stage **(F)**, early-heart stage **(G)**, and mid-heart stage **(H)** are shown.
(I) to **(K)** Photographs of developing *raspberry1* embryos within the same siliques as the wild-type embryos shown in **(F)** to **(H)**.
A, axis; C, cotyledon; EP, embryo proper; Hs, hypophysis; S, suspensor. Bar = 26 μm. The bar in **(K)** applies to all panels.

embryos fail to initiate morphogenetic events at the transition stage that normally result in organ formation and the differentiation of shoot and root meristems.

raspberry Embryos Differentiate Specialized Cell Layers

We utilized in situ hybridization with several cell-specific mRNA markers to determine whether *raspberry* embryos formed specialized tissue layers characteristic of mature wild-type embryos (Figure 1C). Two classes of marker mRNAs were used: (1) a lipid transfer protein mRNA specific for epidermal cells (Sterk et al., 1991; Thoma et al., 1994) and (2) several storage protein mRNAs that accumulate in parenchyma cells (Meyerowitz, 1987; Pang et al., 1988; Guerche et al., 1990; Conceição and Krebbers, 1994). The storage protein mRNA class included the At12S and At2S2 mRNAs, which are represented equally in cotyledon and axis cells, and the At2S1 mRNA, which accumulates preferentially within the axis region (Meyerowitz, 1987; Pang et al., 1988; Guerche et al., 1990). Collectively, these mRNAs enabled us to assay for differentiated epidermal and storage parenchyma cells and, by default, the vascular tissue layer.

Lipid Transfer Protein mRNA Is Localized within the Outer Cell Layer of raspberry *Embryos*

We hybridized an AtLTP1 lipid transfer protein anti-mRNA probe with *raspberry* embryos at different stages of development to determine whether the outer "raspberry-like" cell layer expressed epidermal-specific genes (see Methods). The AtLTP1 mRNA is an Arabidopsis homolog of the carrot EP2 lipid transfer protein mRNA (Sterk et al., 1991; Thoma et al., 1994). Figures 5A to 5G show bright-field photographs of wild-type embryo longitudinal sections at different developmental stages. Figures 5H to 5J show that the AtLTP1 anti-mRNA probe did not produce hybridization signals above background in either the embryo-proper or suspensor regions of wild-type embryos at the globular stage (Figure 5H), heart stage (Figure 5I), or torpedo stage (Figure 5J), even upon long exposures (2.5 months). AtLTP1 mRNA was observed, however, in the outer integument layer of developing seeds containing globular- and heart-stage embryos (Figures 5H and 5I). By contrast, Figures 5K to 5N show that AtLTP1 mRNA was localized specifically within the epidermal cell layer of wild-type embryos from the walking-stick stage (Figure 5K) to the late-maturation stage (Figure 5M). AtLTP1 mRNA was not detectable in the endosperm or other embryo cell types at any stage of development (Figures 5H to 5N). AtLTP1 mRNA levels were similar in cotyledon and axis epidermal cells, except in the root meristem region, which did not have detectable AtLTP1 mRNA (Figures 5K to 5M). Prior to desiccation, AtLTP1 mRNA levels decreased within the epidermal cell layer (Figure 5N).

Figures 5O and 5P show that no detectable AtLTP1 mRNA signal was observed in globular embryos present within young, heterozygous +/*raspberry1* siliques. By contrast, Figures 5Q to 5S show that a strong AtLTP1 hybridization signal was obtained exclusively in the outer cell layer of *both* the embryo-proper and suspensor regions of *raspberry1* embryos. AtLTP1 hybridization grain densities within the *raspberry1* outer cell layer were equal to, or higher than, those observed within the epidermal cells of wild-type, maturation-stage embryos, indicating that AtLTP1 mRNA accumulated to at least the same level in mutant embryos as compared with wild type (e.g., compare Figures 5L and 5R). As shown in Figures 5T and 5U, a similar AtLTP1 mRNA localization pattern was obtained with *raspberry2* embryos. Together, these data indicate that *raspberry* embryos express an epidermal-specific gene expression program within the outer cell layers of both the embryo-proper and suspensor regions and that the temporal regulation of the AtLTP1 gene appears to be unaffected by the *raspberry* mutation.

Storage Protein mRNAs Are Present within the Inner Cell Layers of raspberry *Embryos*

We used several storage protein anti-mRNA probes to determine whether storage parenchyma cells formed in *raspberry* embryos and whether the *raspberry* gene mutations affected the expression of other embryo cell–specific genes. Figure 6 shows the mRNA localization patterns for the At12S storage globulin mRNA (Figures 6A to 6F; Meyerowitz, 1987; Pang et al., 1988), the At2S1 albumin mRNA (Figures 6G to 6L; Guerche et al., 1990; Conceição and Krebbers, 1994), and the At2S2 albumin mRNA (Figures 6M to 6R; Guerche et al., 1990; Conceição and Krebbers, 1994) in wild-type and *raspberry* embryos. The control in situ hybridization experiments with wild-type embryos produced results similar to those obtained by other investigators (Meyerowitz, 1987; Pang et al., 1988; Guerche et al., 1990; Conceição and Krebbers, 1994), except that we extended these data to all embryonic stages. None of the storage protein mRNAs were detected in wild-type embryos prior to the torpedo stage (Figures 6A, 6G, and 6M; and data not shown), even upon very long exposures of the slide emulsion (13 months). Each mRNA began to accumulate in late-torpedo stage embryos. The At2S1 and At2S2 mRNAs accumulated first within the axis region and then within the cotyledons (data not shown). The At12S mRNA, on the other hand, accumulated initially in the upper axis region and then simultaneously in both cotyledons and the remainder of the axis (data not shown). In late-maturation stage embryos, the At12S mRNA was localized specifically within the epidermal and storage parenchyma cell layers (Figures 6B and 6C). No detectable At12S mRNA was observed within vascular tissue (Figures 6B and 6C). The At2S1 and At2S2 mRNAs were localized within the same cell types as the At12S mRNA (Figures 6H, 6I, 6N, and 6O), except that the At2S1 mRNA accumulated

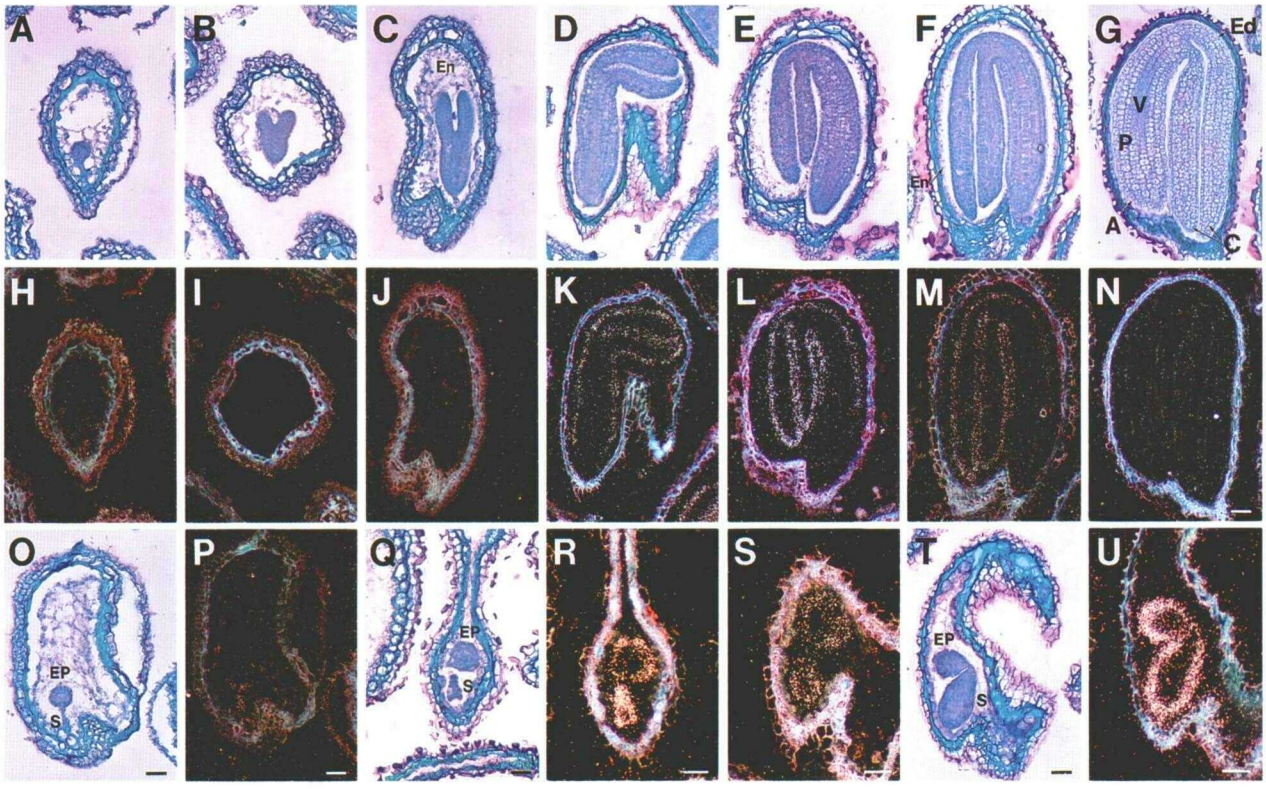

Figure 5. Localization of AtLTP1 Lipid Transfer Protein mRNA in Wild-Type and *raspberry* Embryos.

Seeds were fixed, embedded in paraffin, sliced into sections (6 to 8 μm thick), and hybridized with an AtLTP1 anti-mRNA probe (Sterk et al., 1991; Thoma et al., 1994) as outlined in Methods.

(A) to **(G)** Bright-field photographs of developing wild-type embryos.

(H) to **(N)** Hybridization of the AtLTP1 anti-mRNA probe with wild-type embryos shown in **(A)** to **(G)**. Slide emulsions were exposed for 77 days, and photographs were taken using dark-field microscopy.

(O) and **(Q)** Bright-field photographs of developing *raspberry1* embryos when wild-type embryos within the same silique were in the globular stage **(O)** and the maturation stage **(Q)** of development.

(P), **(R)**, and **(S)** Hybridization of the AtLTP1 anti-mRNA probe with developing *raspberry1* embryos when wild-type embryos within the same silique were at the globular **(P)** and maturation (**[R]** and **[S]**) developmental stages. Photographs were taken using dark-field microscopy. The embryos shown in **(P)** and **(R)** are the same as those shown by bright-field microscopy in **(O)** and **(Q)**, respectively. The embryo shown in **(S)** has no bright-field counterpart. Slide emulsion exposure times were 27 days (**[R]** and **[S]**) and 77 days **(P)**, respectively.

(T) Bright-field photograph of a *raspberry2* embryo at a stage when wild-type embryos within the same silique were at the maturation stage of development.

(U) Hybridization of the AtLTP1 anti-mRNA probe with the *raspberry2* embryo shown in **(T)**. Photograph was taken using dark-field microscopy, and slide emulsion exposure time was 77 days.

A, axis; C, cotyledon; Ed, epidermis; En, endosperm; EP, embryo proper; P, storage parenchyma; S, suspensor; V, vascular tissue. Bar in **(N)** = 37 μm and applies to **(A)** through **(N)**. Bars in **(O)** to **(U)** = 37 μm.

preferentially within the axis and abaxial cell layers of the cotyledons (Figures 6H and 6I). All of the storage protein mRNAs were present within the peripheral endosperm layer of maturing seeds (Figures 6C, 6I, and 6O).

Each storage protein anti-mRNA probe produced a strong hybridization signal with *raspberry1* embryos (Figures 6D, 6E, 6J, 6K, 6P, and 6Q) and *raspberry2* embryos (Figures 6F, 6L, and 6R) at a stage when wild-type embryos within the same silique were in late maturation (Figures 6B, 6C, 6H, 6I, 6N, and 6O). No detectable hybridization grains above background levels were observed with any of the storage protein anti-mRNA probes in *raspberry* embryos early in embryogenesis; that is, all embryos within young heterozygous siliques had background hybridization levels similar to those of the wild-type embryos shown in Figures 6A, 6G, and 6M (and data not shown). Hybridization signals of equal intensity were observed

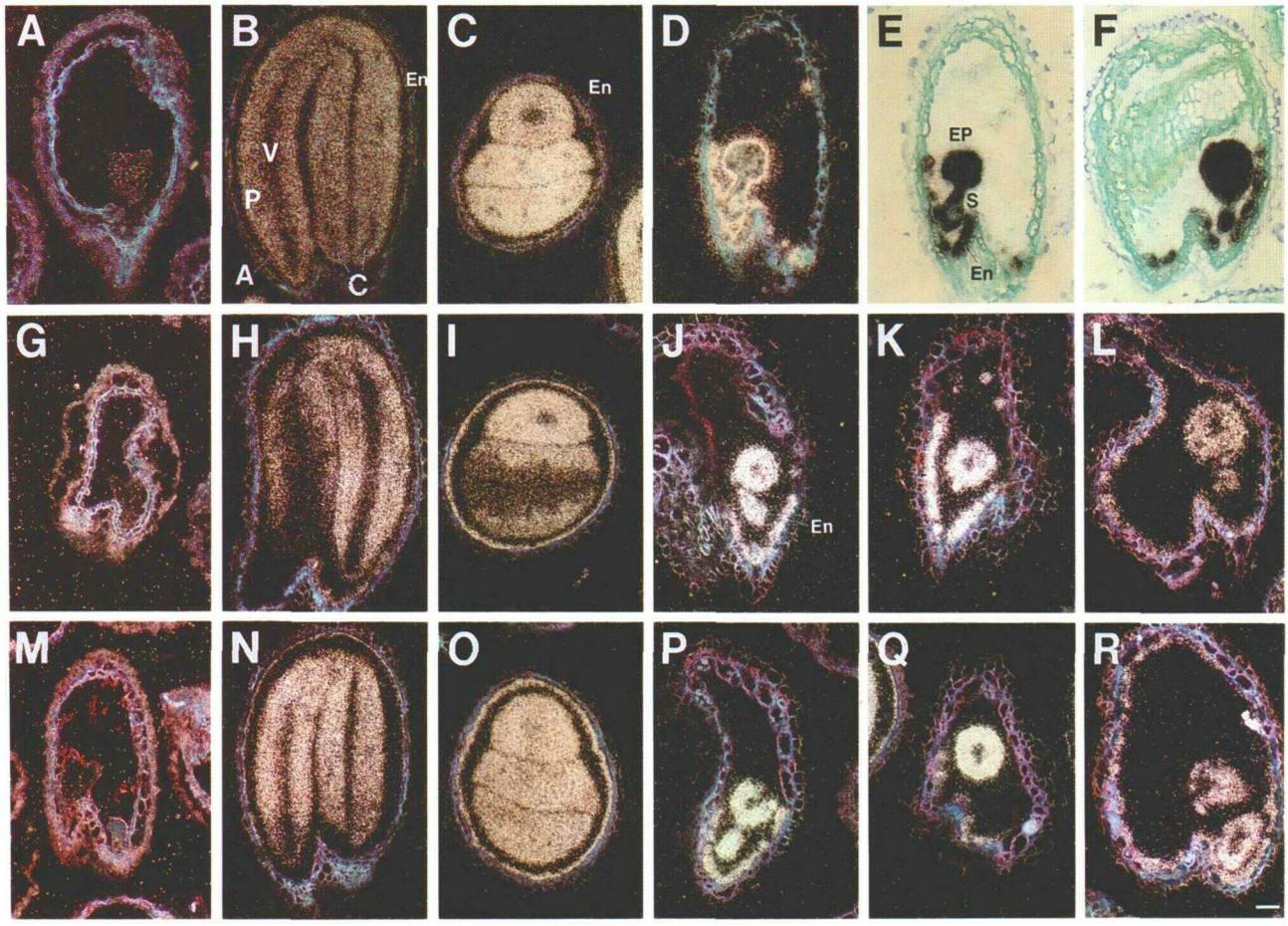

Figure 6. Localization of Storage Protein mRNAs in *raspberry* Embryos.

Seeds were fixed, embedded in paraffin, sliced into sections (6 to 8 μm thick), and hybridized with labeled anti-mRNA probes as outlined in Methods.
(A) to **(C)** Hybridization of an At12S globulin anti-mRNA probe (Meyerowitz, 1987) with seeds containing wild-type embryos at the heart stage **(A)** and late-maturation stage (**[B]** and **[C]**). Slide emulsions were exposed for 3 days **(A)** and 2 days (**[B]** and **[C]**), respectively. Photographs were taken using dark-field microscopy. **(B)** and **(C)** are longitudinal and transverse sections, respectively.
(D) to **(F)** Hybridization of an At12S globulin anti-mRNA probe with *raspberry1* embryos (**[D]** and **[E]**) and a *raspberry2* embryo **(F)** when wild-type embryos within the same silique were in the maturation stage (**[B]** and **[C]**). Slide emulsions were exposed for 3 days (**[D]** and **[E]**) and 5 days **(F)**, respectively. Photographs taken by dark-field microscopy **(D)** and bright-field microscopy (**[E]** and **[F]**).
(G) to **(I)** Hybridization of an At2S1 albumin anti-mRNA probe (Guerche et al., 1990) with seeds containing wild-type embryos at the heart stage **(G)** and late-maturation stage (**[H]** and **[I]**). Slide emulsions were exposed for 21 days **(G)** and 27 days (**[H]** and **[I]**), respectively. Photographs were taken with dark-field microscopy.
(J) to **(L)** Hybridization of an At2S1 anti-mRNA probe with *raspberry1* embryos (**[J]** and **[K]**) and a *raspberry2* embryo **(L)** at a stage when wild-type embryos within the same silique were in late maturation (**[H]** and **[I]**). Slide emulsions were exposed for 27 days, and photographs were taken with dark-field microscopy.
(M) to **(O)** Hybridization of an At2S2 albumin anti-mRNA probe (Guerche et al., 1990) with seeds containing wild-type embryos at the heart stage **(M)** and late-maturation stage (**[N]** and **[O]**). Slide emulsions were exposed for 21 days (**[M]** and **[O]**) and 27 days **(N)**, respectively. Photographs were taken using dark-field microscopy.
(P) to **(R)** Hybridization of an At2S2 anti-mRNA probe with *raspberry1* embryos (**[P]** and **[Q]**) and a *raspberry2* embryo **(R)** at a stage when wild-type embryos within the same silique were in late maturation (**[N]** and **[O]**). Slide emulsions were exposed for 27 days, and photographs were taken by dark-field microscopy.
A, axis; C, cotyledon; Ed, epidermis; En, endosperm; EP, embryo proper; P, storage parenchyma; S, suspensor; V, vascular tissue. Bar = 37 μm. The bar in **(R)** applies to all panels in this figure.

within *both* the embryo-proper and suspensor regions of *raspberry1* and *raspberry2* embryos (Figures 6D to 6F, 6J to 6L, and 6P to 6R). These hybridization signals were equivalent to those observed in wild-type embryos at late maturation (Figures 6B, 6H, and 6N). In addition, strong hybridization of each storage protein anti-mRNA probe occurred with endosperm tissue that remained in late-maturation seeds containing *raspberry* embryos (Figures 6D to 6F, 6J to 6L, and 6P to 6R).

All of the storage protein mRNAs had similar cell localization patterns in the embryo-proper and suspensor regions of *raspberry* embryos—storage protein mRNAs were localized within the outer cell layer and within several inner cell layers, except for a central core region (Figures 6D to 6F, 6J to 6L, 6P to 6R; and data not shown). This cell localization pattern was visualized most clearly in *raspberry2* embryos with the At2S2 mRNA (Figure 6R) and was confirmed with the other storage protein mRNAs by performing in situ hybridization experiments with serial sections through entire *raspberry* embryos (data not shown). Together, these data indicate that several storage protein genes are expressed within the inner cell layers of *raspberry* embryo-proper and suspensor regions and are regulated in time similarly to that observed in wild-type embryos. We conclude from these storage protein mRNA localization data and those obtained for the lipid transfer protein mRNA (Figure 5) that *raspberry* embryos have differentiated epidermal, storage parenchyma, and vascular cell layers and that these layers form in *both* regions of the mutant *raspberry* embryos.

stout and *pump* Embryos Do Not Accumulate Storage Protein mRNAs

We localized storage protein mRNAs in two different embryo-defective mutants, designated as *stout* and *pump*, to determine whether the cell localization patterns observed with the marker mRNAs were specific for *raspberry* embryos or a general feature of all mutants arrested early in embryogenesis (Table 1). We utilized *stout* and *pump* embryos at a stage when wild-type embryos within the same silique were in late maturation for these experiments (Figure 1C). Figures 7A and 7B show that *stout* embryos resembled the wild-type, globular-stage embryo shown in Figure 7C. *stout* embryos did not generate "raspberry-like" protuberances or a highly enlarged suspensor, although enlargement of some suspensor cells did occur (Figure 7B). Figure 7D shows that the At12S anti-mRNA probe did not produce any signal above that of the background control At12S mRNA probe shown in Figure 7E.

In contrast to the spherically shaped *raspberry* and *stout* embryos, Figures 7F and 7G show that *pump* proceeded through the transition stage, initiated cotyledon and axis regions, and was similar in appearance to the wild-type, late-heart stage embryo shown in Figure 7H. No detectable abnormalities were observed within *pump* suspensor regions (Figures 7F and 7G). Figures 7I and 7J show that hybridization of the At2S2 anti-mRNA probe with *pump* embryo longitudinal sections did not reveal any signal above background hybridization levels. Similar results were obtained with the At2S1 and At12S anti-mRNA probes (data not shown). Together, these data indicate that the spatial gene expression patterns observed within *raspberry* embryos are specific for the *raspberry* gene mutations (Figures 5 and 6) and that *stout* and *pump* embryos resemble wild-type embryos at the globular and heart stages with respect to both phenotype and absence of detectable storage protein mRNAs (Figure 6).

DISCUSSION

A Large Number of T-DNA–Tagged Embryo Mutants Have Been Identified

Genetic screens of Arabidopsis families treated with either chemical or T-DNA mutagens have identified a large number of mutants that are arrested at various stages of embryo or seedling development (Feldmann, 1991; Jürgens et al., 1991; Meinke, 1991a, 1991b; Forsthoefel et al., 1992; Castle et al., 1993). Our screen of T-DNA–mutagenized Arabidopsis plants yielded 66 lines (1.1% of the lines screened) that are heterozygous for recessive embryo-defective mutations (Table 1). The embryo-defective mutants that we identified arrest at different stages of embryogenesis and show varying degrees of morphological abnormalities (Table 1). Approximately one-third of the mutants uncovered in our screen are either tagged or tightly linked to the T-DNA. The majority of embryo mutants are globular shaped and fail to initiate cotyledon and axis development (Table 1). Morphological arrest occurred at, or just prior to, the transition from globular stage to heart stage, indicating that this period is particularly sensitive to mutations in a large number of genes. As shown schematically in Figure 8A, this may be due to the fact that a number of critical developmental events occur during the globular/heart transition period, including the differentiation of primary embryonic tissue layers and the initiation of embryonic organs along the radial and longitudinal axes of the embryo proper, respectively (Jürgens et al., 1991; Mansfield and Briarty, 1991; Meinke, 1991b; Goldberg et al., 1994). Our T-DNA screen results are similar to those obtained by Castle et al. (1993), who carried out a parallel screen of different T-DNA–mutagenized Arabidopsis lines in the same greenhouse populations, except that they identified a larger number of embryo-defective mutations (178). Collectively, these T-DNA screens yielded over 240 embryo-defective mutants, of which ~80 have putative T-DNA tags of various complexities (Table 1; Errampalli et al., 1991; Castle et al., 1993).

Morphological Arrest of Embryonic Development at the Globular Stage Often Results in a Raspberry-like Phenotype

Figure 8B summarizes schematically the development of *raspberry1* embryos relative to that of wild-type embryos within

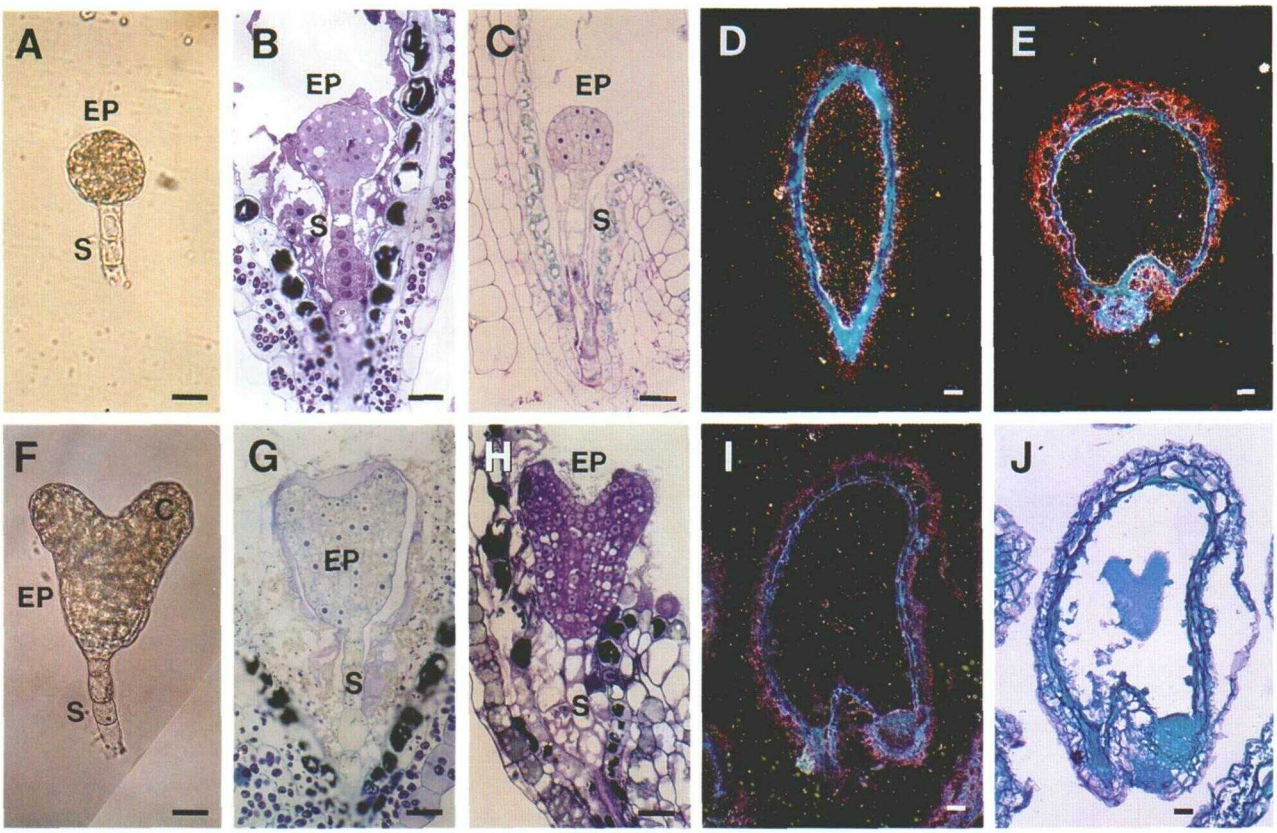

Figure 7. Localization of Storage Protein mRNAs in *stout* and *pump* Embryos.

(A) and **(B)** Bright-field photographs of a whole-mount *stout* embryo **(A)** and a *stout* embryo longitudinal section **(B)**.
(C) Bright-field photograph of a longitudinal section of a wild-type embryo at the mid-globular stage.
(D) and **(E)** Hybridization of an At12S anti-mRNA probe **(D)** and an At12S mRNA probe **(E)** with *stout* embryos. Photographs were taken using dark-field microscopy, and slide emulsion exposure times were for 7 days.
(F) and **(G)** Bright-field photographs of a whole-mount *pump* embryo **(F)** and a *pump* embryo longitudinal section **(G)**.
(H) Bright-field photograph of a longitudinal section of a wild-type embryo at the late-heart stage.
(I) Hybridization of an At2S2 anti-mRNA probe with a *pump* embryo. The photograph was taken using dark-field microscopy. Slide emulsion exposure time was for 21 days.
(J) Bright-field photograph of the *pump* embryo shown in **(I)**.
C, cotyledon; EP, embryo proper; S, suspensor. Bars = 19 μm.

a heterozygous +/*raspberry1* silique (Figure 8A). The early stages of *raspberry1* embryogenesis are indistinguishable from those of wild-type embryos up to the late-globular stage. At our level of resolution, no detectable differences were observed between *raspberry1* and wild-type segregants in either the embryo-proper or suspensor regions prior to the transition stage (Figures 3 and 4). At this period of embryogenesis, a striking change occurs between *raspberry1* and wild-type embryo development (Figures 8A and 8B). In the wild-type embryo-proper region, cotyledons are initiated, hypocotyl elongation begins, the hypophysis undergoes divisions leading to root meristem formation, and the protoderm, ground meristem, and procambium cell layers become distinctly visible—that is, wild-type embryos enter the heart stage (Figure 8A). By contrast, the *raspberry1* embryo-proper region remains globular shaped, the hypophysis does not differentiate into a root meristem, and only a protoderm-like cell layer is visible histologically (Figure 8B). During the later stages of embryogenesis, *raspberry1* embryos enlarge, protuberances form on the outer cell layer, and three specialized tissue layers—epidermis, storage parenchyma, and vascular layer—are differentiated (Figure 8B). In addition, suspensor cell proliferation and the differentiation of embryo-proper–like tissue layers within this region occur (Figure 8B). Thus, *raspberry1* embryogenesis proceeds at the cell differentiation level on a time course similar to that observed in wild-type embryos, except that morphogenetic events leading to bilateral symmetry and organ formation do not take place. *raspberry2* embryos follow a similar series of events, although we have not characterized the precise timing as thoroughly as for *raspberry1*.

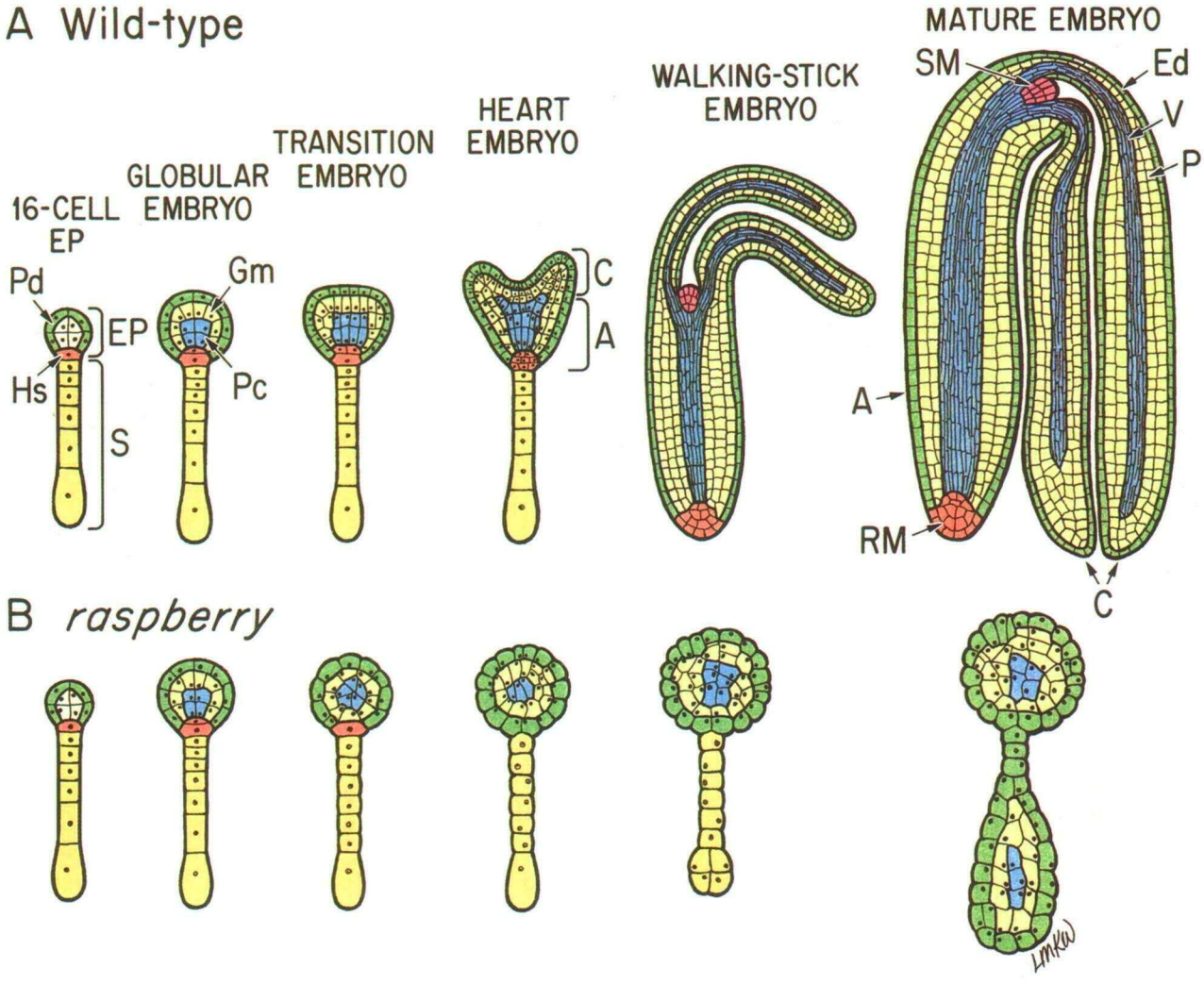

Figure 8. Differentiation of a Radial Tissue–Type Axis in Wild-Type and *raspberry* Embryos.

Colors show the origin and fate of different embryo regions and cell layers. Color coding is the same for wild-type and mutant embryos.
(A) Wild-type embryo development. Based on histological and genetic studies of Arabidopsis embryo development (Mansfield and Briarty, 1991, 1992; Mayer et al., 1991).
(B) *raspberry* embryo development. Inferred from the histological and mRNA localization studies presented in Figures 3 to 6.
A, axis, C, cotyledon, Ed, epidermis; EP, embryo proper; Gm, ground meristem; Hs, hypophysis; P, storage parenchyma; Pc, procambium; Pd, protoderm; RM, root meristem; S, suspensor; SM, shoot meristem; V, vascular tissue.

One intriguing aspect of our results is the large number of globular-shaped mutants that have a "raspberry-like" phenotype (Table 1). Twenty-eight of the 29 mutants arrested at the globular stage have phenotypes resembling those conferred by *raspberry1* and *raspberry2* to varying degrees, including the formation of convex protuberances, cell vacuolization, and elaboration of an enlarged suspensor. Allelism tests and genetic mapping studies carried out thus far on these "raspberry-like" mutants have indicated that they are due to mutations in separate genes (J.K. Okamuro and D.W. Meinke, personal communications). Only one globular-arrested mutant, *stout* (Figure 7A), has a phenotype similar to that of wild-type embryos at the globular stage. Collectively, these results suggest that the vast majority of mutants uncovered as globular arrested are arrested only *morphologically* and that they continue to undergo development and cell differentiation up to the terminal stages of embryogenesis.

What physiological defects are responsible for generating a large number of mutants that fail to undergo morphogenetic events leading to the heart stage? Recent evidence suggests that auxin biosynthesis and polarized transport may play a role in both cotyledon initiation and hypocotyl elongation that leads

to the differentiation of a heart-shaped embryo with bilateral symmetry (Schiavone and Cooke, 1987; Cooke et al., 1993; Liu et al., 1993). Isolated bean embryos have been shown to transport auxin basipetally from the shoot to root meristems of the axis (Fry and Wangermann, 1976). Treatment of carrot somatic embryos with agents that inhibit polarized auxin transport block morphogenetic processes required for the formation of heart-stage embryos and result in the development of giant, globular-shaped embryos (Schiavone and Cooke, 1987). Agents that inhibit polarized auxin transport also prevent normal cotyledon formation and the establishment of bilateral symmetry in cultured Indian mustard zygotic embryos, although a collar-like ring forms around the entire embryo apical region and axis elongation occurs (Liu et al., 1993). These embryos resemble those of the Arabidopsis *pin1-1* mutant, which has a defect in polarized auxin transport (Okada et al., 1991; Liu et al., 1993). In both sets of inhibitor experiments, globular-stage embryos are the ones most sensitive to auxin transport blockers. For example, treatment of heart-stage Indian mustard embryos with agents that prevent polarized auxin transport does not inhibit cotyledon formation (Liu et al., 1993). These results strongly suggest that localized asymmetries in auxin levels are generated within globular-stage embryos and that these asymmetries play a role in orchestrating morphogenetic processes necessary for cotyledon initiation and axis elongation prior to the heart stage (Schiavone and Cooke, 1987; Cooke et al., 1993; Liu et al., 1993). Because a large number of genes are required for auxin biosynthesis, transport, and degradation (Last et al., 1991; Taiz and Zeiger, 1991), mutations in any of these genes might result in a globular-arrested embryo. We suggest, therefore, that the number of globular-arrested mutants might be due, in part, to defects in auxin transport and/or metabolism during the early stages of embryogenesis.

raspberry Suspensors Differentiate Embryo-Proper–like Tissue Layers

In contrast to the defects observed in embryo-proper morphogenesis, a normal-looking suspensor forms during the early stages of *raspberry1* embryogenesis (Figures 3 and 4). No apparent differences were observed between *raspberry1* and wild-type suspensor regions up to at least the heart stage, even though the *raspberry1* embryo proper remains globular shaped (Figures 8A and 8B). This result indicates that the *raspberry1* mutation does not impair events leading to suspensor differentiation.

At the later stages of *raspberry1* embryogenesis, a striking change occurs within the suspensor region (Figures 1G to 1I). Cells at the basal end of the suspensor divide and proliferate an enlarged, multicellular structure that bulges outward in a polarized direction away from the abnormal embryo-proper region (Figures 1G to 1I). Surprisingly, mRNAs that are markers for embryo-proper cell types accumulate within specific cell layers of the enlarged *raspberry1* suspensor region in their correct spatial contexts (Figures 5, 6, 8A, and 8B). This suggests that the enlarged suspensor differentiates an embryo-proper–like radial tissue–type axis and takes on an embryo-proper–like identity. Because a similar result was obtained with *raspberry2* embryos (Figures 5 and 6), the differentiation of an embryo-proper–like radial tissue–type axis probably occurs generally within the abnormal suspensors of many globular-arrested mutants.

The mechanism by which an embryo-proper–like radial tissue axis is established within *raspberry* suspensors is not known. However, the process by which the mutant suspensor region achieves its radial tissue pattern is clearly different from how this occurs during the early stages of embryogenesis within the embryo-proper region (Figure 8A). The stereotyped cell division patterns observed during early embryo–proper development differ from those that take place in *raspberry* suspensors during the late stages of embryogenesis. The ultimate result, however, with respect to the differentiation and positioning of specialized tissue layers along the radial axis is the same. This suggests that interactions may occur between differentiating epidermal, ground meristem, and vascular cell layers and that these interactions lead to a stereotyped pattern of radial tissue organization, irrespective of the pathway by which this process is triggered.

Ablation experiments have shown that destruction of the embryo proper results in the induction of an embryo-proper–like pathway in the terminally differentiated suspensor cells (Haccius, 1963). This result demonstrates that interactions occur between the embryo-proper and suspensor regions and that the presence of a normal embryo proper suppresses the induction of an embryo-proper–like pathway within the suspensor (Haccius, 1963). In addition to *raspberry1* and *raspberry2*, a large number of Arabidopsis recessive mutations have been identified that lead to enlarged, abnormal suspensor regions (Marsden and Meinke, 1985; Castle et al., 1993; Yeung and Meinke, 1993; Schwartz et al., 1994). In each case, morphogenetic defects occur within the embryo proper, suggesting that a signal repressing the embryo-proper pathway in suspensor cells has been disrupted (Schwartz et al., 1994). Mutant embryos that have normal embryo-proper regions, but arrest at specific embryonic stages, do not have aberrant suspensors (R. Yadegari, G.R. de Paiva, T. Laux, A.M. Koltunow, N. Apuya, J.L. Zimmerman, R.L. Fischer, J.J. Harada, and R.B. Goldberg, unpublished data). How the embryo-proper and suspensor regions communicate with each other remains to be determined. Because the embryo-proper ablation experiments (Haccius, 1963) and mutations that cause defects in embryo-proper morphogenesis both result in the induction of an embryo-proper–like pathway in the suspensor, genes such as *raspberry1* and *raspberry2* probably exert their effect primarily within the embryo-proper region.

raspberry Embryo Cell Differentiation Occurs in the Absence of Morphogenesis

A major conclusion of the experiments presented here is that specialized cell layers characteristic of embryos at the terminal

stages of development can differentiate within an embryo that fails to form embryonic organs (Figure 8B). That is, embryo cell specialization can occur in the absence of morphogenetic events leading to axis and cotyledon formation. *raspberry* embryos accumulate cell-specific mRNAs in a spatial pattern similar to that found in the axis and cotyledons of late-maturation stage, wild-type embryos (Figures 5 and 6). In addition, *raspberry* embryos have cellular features of wild-type embryos at late maturation, such as convex protuberances on their outer surfaces and prominent intracellular vacuoles (Figures 1 and 2). These results indicate that the three primordial tissue layers that are specified in *raspberry* embryos at the globular stage continue to develop and follow a specialization pathway that leads to the expression of markers characteristic of the late stages of embryogenesis (Figure 8B). A similar conclusion has been inferred from histological examination of Arabidopsis *sus* mutants that have phenotypes that closely resemble those conferred by *raspberry1* and *raspberry2* (Schwartz et al., 1994). Cell differentiation, therefore, can be uncoupled from morphogenesis in a plant embryo, implying that morphogenetic checkpoints do not have to occur before cell specialization events can proceed (Losick and Shapiro, 1993). This result implies that a radial tissue–type axis can form during embryogenesis irrespective of events leading to the elaboration of embryonic structures along the longitudinal shoot/root axis.

How primary embryonic cell layers form during plant embryogenesis is not known. Our data suggest, however, that once specified these cell layers follow an internal developmental clock that controls the manifestation of specialized functions in an appropriate temporal context. For example, storage protein and lipid transfer protein mRNAs accumulate in *raspberry* embryos during the same embryonic period as they do in the axis and cotyledon cells of wild-type embryos (Figures 5 and 6). Thus, each *raspberry* embryonic cell layer can "sense" the appropriate developmental time to differentiate specialized functions characteristic of embryos at the late stages of embryogenesis, even though these layers are not part of an elaborate organ system. An important corollary is that the *raspberry* gene mutations do not appear to affect the regulatory circuitry of several different genes that are transcribed during late maturation.

Mutations that affect embryo cell specification events can cause defects to occur in morphogenetic processes. For example, Arabidopsis *knolle* embryos lack an epidermal cell layer and have a ball-like shape without defined organ systems or apical and basal regions (Jürgens et al., 1991; Mayer et al., 1991). Similarly, the carrot *ts11* somatic embryo mutant has a defective protoderm layer and remains globular shaped (De Jong et al., 1993). *ts11* embryo mutants can be rescued by the addition of *Rhizobium* lipooligosaccharide nod factors, which have been shown to act as signaling molecules in root nodule induction (Lerouge et al., 1990; De Jong et al., 1993). These results suggest that protoderm signals may be required for normal morphogenesis to occur during embryo development and that cells within the radial tissue–type axis may interact with each other. The data presented here indicate that defects in morphogenesis can also occur in embryos that specify all primordial tissue layers correctly. The nature of *raspberry* genes and how they affect morphogenetic processes during embryo development remain to be determined.

METHODS

Mutant Isolation and Genetic Analyses

Five thousand eight hundred twenty-two T-DNA–mutagenized lines of *Arabidopsis thaliana* ecotype Wassilewskija (WS) were screened for embryo mutants at the Du Pont Experimental Station (Wilmington, DE, in November 1990) and at the University of Arizona (Tucson, in November 1991) (Feldmann and Marks, 1987; Errampalli et al., 1991; Feldmann, 1991; Forsthoefel et al., 1992; Castle et al., 1993). Embryo mutants were identified within the immature siliques of six to eight T_3 plants by scoring for a 3:1 ratio of wild-type to defective T_4 seeds (Meinke and Sussex, 1979). Recessive embryo mutants were maintained as heterozygotes that produced 25% mutant embryos upon self-pollination. Mutant phenotypes were characterized by dissecting immature seeds and examining whole-mount embryos using dissecting and compound microscopes.

Light Microscopy

Mutant and wild-type seeds were embedded in Spurr's epoxy resin (Spurr, 1969), sliced into sections (1 to 2 μm thick) using a microtome (LKB Ultratome V; LKB, Bromma, Sweden), and then stained overnight with 0.2 to 0.5% toluidine blue. Bright-field photographs were taken with Kodak Gold 100 film (ISO 100/21°) using a compound microscope (Olympus BH-2; Olympus Corporation, Lake Success, NY).

Nomarski photographs of whole-mount embryos were obtained by fixing longitudinally slit siliques in an ethanol:acetic acid (9:1) solution overnight, followed by two washes in 90% and 70% ethanol, respectively. Siliques were cleared with a chloral hydrate:glycerol:water solution (8:1:2, w:v:v), and the seeds were dissected prior to microscopy (Berleth and Jürgens, 1993). Embryos were visualized using a Zeiss Axiophot (Carl Zeiss, Inc., Oberkochen, Germany) or an Olympus BH-2 microscope equipped with Nomarski optics. Photographs were taken using Kodak TMAX 100 (E.I. 100/21°) film.

Bright-field photographs of whole-mount embryos were obtained by immersing hand-dissected embryos in water and then photographing the embryos with Kodak Gold 100 film (ISO 100/21°) using a Zeiss Axiophot or Olympus BH-2 microscope.

Scanning Electron Microscopy

Wild-type and mutant embryos were prepared for scanning electron microscopy according to the procedure of Irish and Sussex (1990) with modifications. Hand-dissected embryos were fixed in a capillary chamber containing FAA (50% ethanol, 5% acetic acid, 3.7% formaldehyde) for 48 hr at room temperature. Embryos were later dehydrated in a graded ethanol series and critical point dried in liquid CO_2. Individual embryos were then placed on scanning electron microscope stubs and coated with paladium–gold in a sputter coater (Hummer, Alexandria, VA). Samples were examined in an autoscan scanning electron microscope (ETEC Corporation, Hayward, CA) with an acceleration voltage of 10 kV. Photographs were taken using Polaroid type 55 film.

Transmission Electron Microscopy

Wild-type and mutant seeds were fixed in 5% glutaraldehyde, 0.1 M phosphate buffer, 0.01% Triton X-100 for 16 hr at 4°C. Seeds were later washed three times in phosphate buffer and post-fixed in 2% osmium tetroxide, followed by dehydration in a graded ethanol series. Samples were embedded in Spurr's epoxy resin (Spurr, 1969; Ted Pella, Inc., Redding, CA), sliced into sections (60 to 100 nm thick), and stained with lead citrate and uranyl acetate. Embryo sections were visualized with a Zeiss 10C electron microscope and photographed with Kodak Electron Microscope Film (No. 4489).

In Situ Hybridization Studies

In situ hybridization studies were carried out as described by Cox and Goldberg (1988) with minor modifications. In brief, individual seeds were harvested from siliques and fixed immediately in a phosphate-buffered glutaraldehyde solution (Meyerowitz, 1987) for 3 to 4 hr. Fixed seeds were dehydrated, cleared, embedded in paraffin, and sliced into sections (6 to 8 μm thick) as described by Cox and Goldberg (1988). Seed sections were mounted on precoated slides (Fisher Superfrost/Plus; Fisher Scientific, Pittsburgh, PA), deproteinized to increase accessibility of the target RNA, and acetylated to reduce nonspecific background prior to hybridization. No prior coating of the sections with BSA or other blocking agents was performed. ^{35}S-labeled anti-mRNA probes of $\geq 1 \times 10^9$ dpm/μg specific activity were hydrolyzed to a modal size of 75 to 100 bases and then hybridized with the sections for 15 to 17 hr at a 42°C, 0.3 M Na^+, 50% formamide hybridization criterion in a humid chamber. After hybridization, the seed sections were incubated with RNase A and washed at a 57°C, 0.02 M Na^+ criterion. Slides containing hybridized seed sections were coated with nuclear track emulsion (Kodak NTB2), exposed for up to 13 months, developed, and then stained with 0.05% toluidine blue. As a control for nonspecific hybridization, a sense RNA probe was hybridized to seed sections exactly as previously described. Photographs were taken with Kodak Gold 100 film (ISO 100/21°) using an Olympus BH-2 microscope with either bright-field or dark-field illumination. Color prints were produced by Village Photo (Westwood, CA) using a standard automated developing and printing process.

ACKNOWLEDGMENTS

We thank Minh Huynh, Sharon Hue Tu, and Birgitta Sjostrand for help with the sectioning and microscopy studies; Margaret Kowalczyk for preparing the figures; and Bonnie Phan for typing this manuscript. We are grateful to Dr. Ken Feldmann for allowing us to screen his T-DNA–mutagenized Arabidopsis lines, and to Drs. Sacco de Vries, Enno Krebbers, and Elliot Meyerowitz for the Arabidopsis cell–specific mRNA probes. We especially thank all of the individuals within the Embryo 21st Century Project laboratories (R.B.G, A.M.K., R.L.F., J.J.H., and J.L.Z.) for stimulating discussions and help in carrying out this research.

Received October 13, 1994; accepted October 19, 1994.

REFERENCES

Berleth, T., and Jürgens, G. (1993). The role of *monopteros* in organizing the basal body region of the *Arabidopsis* embryo. Development **118,** 575–587.

Castle, L.A., Errampalli, D., Atherton, T.L., Franzmann, L.H., Yoon, E.S., and Meinke, D.W. (1993). Genetic and molecular characterization of embryonic mutants identified following seed transformation in *Arabidopsis.* Mol. Gen. Genet. **241,** 504–514.

Conceição, A. da S., and Krebbers, E. (1994). A cotyledon regulatory region is responsible for the different spatial expression patterns of *Arabidopsis* 2S albumin genes. Plant J. **5,** 493–505.

Cooke, T.J., Racusen, R.H., and Cohen, J.D. (1993). The role of auxin in plant embryogenesis. Plant Cell **5,** 1494–1495.

Cox, K.H., and Goldberg, R.B. (1988). Analysis of plant gene expression. In Plant Molecular Biology: A Practical Approach, C.H. Shaw, ed (Oxford: IRL Press), pp. 1–34.

De Jong, A.J., Heidstra, R., Spaink, H.P., Hartog, M.V., Meijer, E.A., Hendricks, T., Lo Schiavo, F., Terzi, M., Bisseling, T., Van Kammen, A., and De Vries, S.C. (1993). *Rhizobium* lipooligosaccharides rescue a carrot somatic embryo mutant. Plant Cell **5,** 615–620.

Errampalli, D., Patton, D., Castle, L., Mickelson, L., Hansen, K., Schnall, J., Feldmann, K., and Meinke, D. (1991). Embryonic lethals and T-DNA insertional mutagenesis in *Arabidopsis.* Plant Cell **3,** 149–157.

Feldmann, K.A. (1991). T-DNA insertion mutagenesis in *Arabidopsis*: Mutational spectrum. Plant J. **1,** 71–82.

Feldmann, K.A., and Marks, M.D. (1987). *Agrobacterium*-mediated transformation of germinating seeds of *Arabidopsis thaliana*: A non-tissue culture approach. Mol. Gen. Genet. **208,** 1–9.

Forsthoefel, N.R., Wu, Y., Schulz, B., Bennett, M.J., and Feldmann, K.A. (1992). T-DNA insertion mutagenesis in *Arabidopsis*: Prospects and perspectives. Aust. J. Plant Physiol. **19,** 353–366.

Fry, S.C., and Wangermann, E. (1976). Polar transport of auxin through embryos. New Phytol. **77,** 313–317.

Goldberg, R.B., Barker, S.J., and Perez-Grau, L. (1989). Regulation of gene expression during plant embryogenesis. Cell **56,** 149–160.

Goldberg, R.B., De Paiva, G., and Yadegari, R. (1994). Plant embryogenesis: Zygote to seed. Science **266,** 605–614.

Guerche, P., Tire, C., Grossi de Sa, F., De Clercq, A., Van Montagu, M., and Krebbers, E. (1990). Differential expression of the *Arabidopsis* 2S albumin genes and the effect of increasing gene family size. Plant Cell **2,** 469–478.

Haccius, B. (1963). Restitution in acidity-damaged plant embryos—regeneration or regulation? Phytomorphology **13,** 107–115.

Irish, V.F., and Sussex, I.M. (1990). Function of the *apetala-1* gene during *Arabidopsis* floral development. Plant Cell **2,** 741–753.

Jürgens, G., Mayer, U., Torres-Ruiz, R.A., Berleth, T., and Miséra, S. (1991). Genetic analysis of pattern formation in the *Arabidopsis* embryo. Development **1** (suppl.), 27–38.

Last, R.L., Bissinger, P.H., Mahoney, D.J., Radwanski, E.R., and Fink, G.R. (1991). Tryptophan mutants in *Arabidopsis*: The consequences of duplicated tryptophan synthase β genes. Plant Cell **3,** 345–358.

Lerouge, P., Roche, P., Faucher, C., Maillet, F., Truchet, G., Promé, J.C., and Dénarié, J. (1990). Symbiotic host-specificity of *Rhizobium*

meliloti is determined by a sulfated and acetylated glucosamine oligosaccharide signal. Nature **344,** 781–784.

Liu, C.-m., Xu, Z.-h., and Chua, N.-H. (1993). Auxin polar transport is essential for the establishment of bilateral symmetry during early plant embryogenesis. Plant Cell **5,** 621–630.

Losick, R., and Shapiro, L. (1993). Checkpoints that couple gene expression to morphogenesis. Science **262,** 1227–1228.

Mansfield, S.G., and Briarty, L.G. (1991). Early embryogenesis in *Arabidopsis thaliana*. II. The developing embryo. Can. J. Bot. **69,** 461–476.

Mansfield, S.G., and Briarty, L.G. (1992). Cotyledon cell development in *Arabidopsis thaliana* during reserve deposition. Can. J. Bot. **70,** 151–164.

Marsden, M.P.F., and Meinke, D.W. (1985). Abnormal development of the suspensor in an embryo-lethal mutant of *Arabidopsis thaliana*. Am. J. Bot. **72,** 1801–1812.

Mayer, U., Torres-Ruiz, R.A., Berleth, T., Miséra, S., and Jürgens, G. (1991). Mutations affecting body organization in the *Arabidopsis* embryo. Nature **353,** 402–407.

Meinke, D.W. (1991a). Embryonic mutants of *Arabidopsis thaliana*. Dev. Genet. **12,** 382–392.

Meinke, D.W. (1991b). Perspectives on genetic analysis of plant embryogenesis. Plant Cell **3,** 857–866.

Meinke, D.W., and Sussex, I.M. (1979). Embryo-lethal mutants of *Arabidopsis thaliana*. Dev. Biol. **72,** 50–61.

Meyerowitz, E.M. (1987). *In situ* hybridization to RNA in plant tissue. Plant Mol. Biol. Rep. **5,** 242–250.

Okada, K., Oeda, J., Komaki, M.K., Bell, C.J., and Shimura, Y. (1991). Requirement of the auxin polar transport system in early stages of *Arabidopsis* floral bud formation. Plant Cell **3,** 677–684.

Pang, P.P., Pruitt, R.E., and Meyerowitz, E.M. (1988). Molecular cloning, genomic organization, expression and evolution of 12S seed protein genes of *Arabidopsis thaliana*. Plant Mol. Biol. **11,** 805–820.

Perez-Grau, L., and Goldberg, R.B. (1989). Soybean seed protein genes are regulated spatially during embryogenesis. Plant Cell **1,** 1095–1109.

Raven, P.H., Evert, R.F., and Eichorn, S.E. (1992). Biology of Plants. (New York: Worth).

Schiavone, F.M., and Cooke, T.J. (1987). Unusual patterns of somatic embryogenesis in the domesticated carrot: Developmental effects of exogenous auxins and auxin transport inhibitors. Cell Differ. **21,** 53–62.

Schwartz, B.W., Yeung, E.C., and Meinke, D.W. (1994). Disruption of morphogenesis and transformation of the suspensor in abnormal *suspensor* mutants of *Arabidopsis*. Development, in press.

Spurr, A.R. (1969). A low viscosity epoxy embedding medium for electron microscopy. J. Ultrastruct. Res. **26,** 31–43.

Sterk, P., Booij, H., Schellekens, G.A., Van Kammen, A., and De Vries, S.C. (1991). Cell-specific expression of the carrot EP2 lipid transfer protein gene. Plant Cell **3,** 907–921.

Taiz, L., and Zeiger, E. (1991). Plant Physiology. (New York: Benjamin/Cummings).

Thoma, S., Hecht, U., Kippers, A., Botella, J., DeVries, S., and Somerville, C. (1994). Tissue-specific expression of a gene encoding a cell wall-localized lipid transfer protein from *Arabidopsis*. Plant Physiol. **105,** 35–45.

Yeung, E.C., and Meinke, D.W. (1993). Embryogenesis in angiosperms: Development of the suspensor. Plant Cell **5,** 1371–1381.